

## Research Article

# Study on Deterioration Effect of Dynamic Mechanical Properties of Granite at Subzero Temperatures

Yang Yang<sup>1</sup> and Jianguo Wang<sup>2</sup>

<sup>1</sup>School of Civil and Recourses Engineering, University of Science and Technology Beijing, Beijing 100083, China

<sup>2</sup>Faculty of Land Resources Engineering, Kunming University of Science and Technology, Kunming, 650093 Yunnan, China

Correspondence should be addressed to Jianguo Wang; wangjg0831@163.com

Received 14 February 2022; Revised 23 March 2022; Accepted 13 June 2022; Published 28 June 2022

Academic Editor: Zhongguang Sun

Copyright © 2022 Yang Yang and Jianguo Wang. This is an open access article distributed under the Creative Commons Attribution License, which permits unrestricted use, distribution, and reproduction in any medium, provided the original work is properly cited.

In the present work, through the dynamic impact test of frozen granite, the effect of temperature on the dynamic mechanical performances of granite at high strain rates were investigated. Based on the existing energy and damage theory, the effects of different low temperatures on the energy dissipation, damage variables, and strength of red sandstone are explored. The reasons for the deterioration of granite dynamic mechanical strength at low temperature are studied by combining analyses of fracture morphology. Researched results showed that low temperatures ( $<-20^{\circ}\text{C}$ ) cause “frostbite” in granite, leading to the sharp decrease of dynamic and macromechanical strength of the rock under a high strain. Under this dynamic disturbance, transient engineering disasters are easy to occur. The analysis of fracture morphology showed that the lower negative temperature results in the formation of cracks among the mineral particles in the granite. Under high strain rate loading, these cracks have poor plastic deformation ability and are easily destabilized and expanded. Moreover, frozen granite tends to be brittle as a whole. With the decrease of negative temperature, its fracture behavior gradually changes from cleavage fracture to transgranular fracture, and the failure mode also changes from tensile failure to shear failure. The coupling effect of impact and the lower negative temperature will cause the quasicleavage of some crystalline minerals, eventually leading to low-stress brittle failure of granite.

## 1. Introduction

There exist evident differences between the mechanical performances of rocks at a normal temperature and the rock mechanical performances at negative temperature, particularly the negative temperature under the condition of dynamic mechanical properties, which frequently exhibit extremely special mechanical response characteristics [1, 2], and, as the cold area of geotechnical engineering and artificial freezing technology have advanced, the rock mechanical properties in a negative temperature state have gradually become a subject of academic study. Researchers all over the world have studied the mechanical properties of rock under negative temperatures to a certain extent. For instance, Aoki et al. [3] implemented the Brazilian splitting test and quasi-static uniaxial compression test on various rocks in a negative temperature zone. The outcomes exhibit that the

elastic modulus and compressive tensile strength of the rocks raised evidently under a temperature of  $-160^{\circ}\text{C}$ . In addition, Yamabe and Neaupane [4] detected the static performances of the sandstone at a negative temperature through triaxial and uniaxial studies and observed that the compressive strength and tensile strength of sandstone raised as the temperature reduces, which was in accordance with the law of former researches. Nonetheless, the elastic modulus remained constant between  $-10^{\circ}\text{C}$  and  $-20^{\circ}\text{C}$  and was little influenced via temperature. Dwivedi et al. [5] detected the fracture toughness of eight types of the rocks under a low temperature through employing Brazilian disk experiment again. It was observed that the rock fracture toughness at a negative temperature was markedly greater, in contrast to at normal temperature, and exhibited a linear growth correlation as the temperature reduces. Tang et al. and Yang et al. [6–10] explored the mechanical

performances of various rocks under a negative temperature (between  $-10^{\circ}\text{C}$  and  $-50^{\circ}\text{C}$ ) through quasistatic and static mechanical experiments. The research outcomes [11–16] suggest that the negative temperature possesses a great impact on the rock mechanical parameters, and the compressive strength, elastic modulus, cohesion, and internal friction angle of the rock raise with the reducing temperature. They attributed the increase of mechanical properties with decreasing temperature to the contraction of mineral particles at negative temperature, the increase of ice strength, and the interaction between frost heaving force and rock. Although these studies have initially revealed the strength characteristics of frozen rock under quasistatic conditions, there are still some limitations [17–20]. This is because, in the process of geotechnical engineering construction, there are often accompanied by dynamic load disturbances such as explosion and impact, but so far, there are almost no researches on dynamic mechanical performances of frozen rock under strong disturbance.

As a result, in the current work, the experimental system of split Hopkinson pressure bar (SHPB) was utilized to conduct a negative temperature impact test on granite. The dynamic mechanical performances of frozen granite under impact were studied. The test temperature varied widely from  $25^{\circ}\text{C}$  to  $-40^{\circ}\text{C}$ , which comprehensively describes the influence of negative temperature on rock dynamic behavior. Combined with scanning electron microscopy, the microscopic fracture characteristics of frozen rock were accurately characterized by fracture morphology analysis. On this basis, the effects of water-ice phase transition and negative temperature on the rock deformation features and dynamic mechanical strength were explored.

## 2. Dynamic Impact Experiment of Frozen Granite

*2.1. Specimen Preparation and Basic Physical Parameters.* Granite blocks with good integrity and homogeneity were selected from Fangshan quarry as research material. According to the requirements of SHPB test system, the rock block was cored, cut, polished, and polished into the  $\Phi 74 \times 38$  mm cylindrical specimens. The nonparallelism of the axial direction and end face of specimen shall be controlled within 0.02 mm. Figure 1 shows some prepared specimens.

The test will employ two types of specimens: dry and saturated. The dry specimen is baked at  $105^{\circ}\text{C}$  for 48 h until its weight is constant (its mass change within 24 h is not more than 0.1%) and then stored in the drying dish. For the water-saturated specimen, place the dried sample in the vacuum water saturator and extract the air in a container under 0.1 MPa of pressure; after air extraction for two hours, inject distilled water into a container; prepare the water surface above the sample and pump air for four hours before no bubbles overflow, after which it stood for 48 hours at atmospheric pressure. The fundamental physical parameters for the two samples determined via the instruments are reflected in Table 1.



FIGURE 1: Prepared granite specimen.

TABLE 1: Basic physical parameters of granite.

Rock type	Velocity of longitudinal wave $\text{m}\cdot\text{s}^{-1}$		Dry density $\text{kg}\cdot\text{m}^{-3}$	Saturated density $\text{kg}\cdot\text{m}^{-3}$	Saturation rate %
	Dry	Saturated			
Granite	3788	4519	2889	2903	0.41

*2.2. Experimental Scheme.* The dynamic impact test was implemented through utilizing a SHPB compression bar test device with a large diameter of 75 mm (see Figure 2), and the research object was water-saturated granite frozen under different negative temperature conditions. Frozen rock specimens were prepared in a high- and low-temperature testing machine (see Figure 3); seven temperature grades were set up in the test, namely,  $-5^{\circ}\text{C}$ ,  $-10^{\circ}\text{C}$ ,  $-15^{\circ}\text{C}$ ,  $-20^{\circ}\text{C}$ ,  $-30^{\circ}\text{C}$ ,  $-40^{\circ}\text{C}$ , and  $25^{\circ}\text{C}$ , respectively. After specimens were placed in the testing machine, it can be used for dynamic impact test only after they were kept constant at the corresponding temperature at least 24 h. To ensure the constant negative temperature condition throughout the test process, the system of SHPB pressure bar test was added with temperature compensation device. The temperature compensation device is designed to maintain the temperature of the frozen rock during the test by generating low temperatures through liquid nitrogen and weak the influence of room temperature fluctuation. The tests were divided into 7 groups according to temperature gradient, with at least 3 specimens in each group. After low temperature treatment, the specimens were quickly transferred to the SHPB compression bar test device with a large diameter of 75 mm, and the uniaxial impact test of frozen granite specimens at low temperatures was completed by applying 0.72 MPa gas pressure.

Because of the nonuniform and noncontinuous nature of the rock, a biconical impact bar is chosen for creating an incident wave with long rising period and gentle rising edge, so as to ensure the stress balance of rock samples during loading [11, 12]. Between the two cones, cylindrical segments of proper length were added. As exhibited in Figure 2, the biconical impact bar was utilized, and the rear and front cone lengths are 130 and 310 mm, and the middle cylinder length is 100 mm.

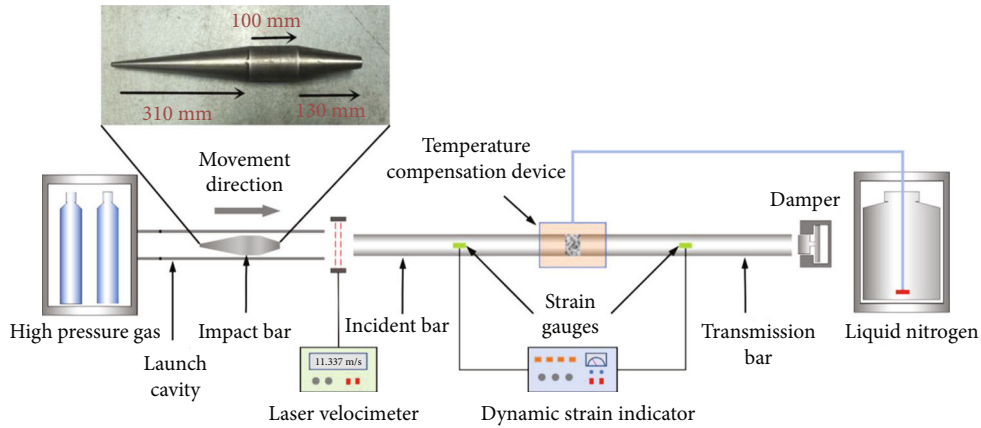


FIGURE 2: Split Hopkinson pressure bar with a temperature compensation device.



FIGURE 3: High- and low-temperature testing machine.

The incident waves formed through conical biconical impact rod are sinusoidal harmonics, which can afford sufficient rise time, and simultaneously eliminate the oscillation existed in waveform curve. The longer rise time facilitates the sample dynamic stress balance and ensures the reliability of the experimental outcomes. In Figure 4, the voltage value of reflected wave and incident wave after the superposition is in good agreement with the voltage value of transmitted wave, reflecting that the rock specimen is in the dynamic stress equilibrium and the experimental outcomes are reliable.

### 3. Dynamic Mechanical Properties of Granite under Different Negative Temperature

**3.1. Analysis of Stress-Strain Curves.** To examine stress-strain characteristics, typical curves were chosen (see Figure 5). Here has the temperature varies from 25°C to -10°C; the values of peak stress and initial elastic modulus are almost the same. However, with the decrease of temperature, the values of failure strain decrease regularly, and the nonlinear variation section of the curve becomes shorter, indicating that granite gradually loses toughness and tends to brittleness under negative temperature. Also, after -20°C, the initial elastic modulus of granite declines, and the peak stress also decreases slightly. However, at -30°C, the initial elastic modulus and peak stress decrease greatly, and the fail-

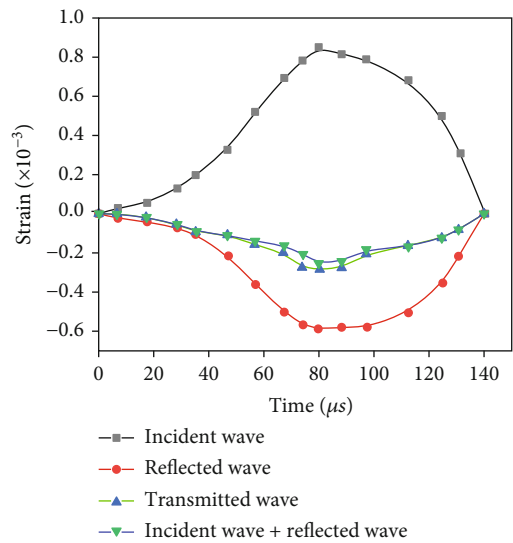


FIGURE 4: Dynamic typical waveform and verification of stress balance.

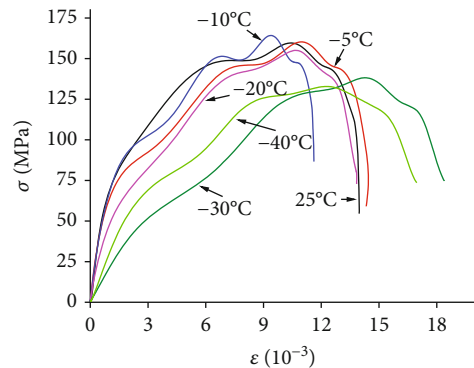


FIGURE 5: Stress-strain curve of granite under impact load.

ure strain increases sharply, so the whole curve appears long and flat. The stress-strain curve at -40°C is similar to that at -30°C, but the peak stress decreases further.

The stress-strain curve analysis presented above shows that “frostbite” occurs in granite when the temperature

drops to  $-30^{\circ}\text{C}$ , that is, the dynamic mechanical performances of the granite deteriorate. This is because a large number of microcracks occur in negative temperature rock under high strain rate loading. These damage and microcracks are not sensitive to static or static loading and therefore have little effect on static strength. However, a high strain rate will amplify its effect, resulting in deterioration of rock mechanical properties and a sharp decrease of dynamic mechanical strength.

*3.2. Macroscopic Failure Characteristics and Dynamic Mechanical Characteristics.* Figure 6 shows the failure modes of water-saturated granite under strong impact at various temperatures. From the figure, it can be found that the damage of rock occurs at various temperatures, but there are evident differences in morphology and blockiness of broken bodies.

- (1) Under a temperature of  $25^{\circ}\text{C}$ , the specimen was subjected to a strong axial compression under the effect of the compressive stress wave. The rock expanded radially and local failure occurred. The local broken body was between the lamellar and columnar splitting structure, which was caused by tension
- (2) At  $-5^{\circ}\text{C}$ , rock brittleness is enhanced, and deformation resistance is reduced at negative temperature. Under the effect of compressive stress wave, the specimen is easy to form columnar splitting structure along the axial direction, and the fracture angle is about  $110^{\circ}$ , which is a typical tensile fracture
- (3) At  $-10^{\circ}\text{C}$ , the rock tends to shrink at negative temperatures, and its resistance to radial expansion deformation is enhanced. The granite remains intact under the impact, and some specimens have tiny cracks
- (4) At  $-15^{\circ}\text{C}$ , the negative temperature further decreases, and the rock's resistance to radial shrinkage deformation begins to decline. Under the action of reverse tensile wave (which causes the radial rebound of the rock specimen), the lamination failure occurs
- (5) From  $-20^{\circ}\text{C}$  to  $-40^{\circ}\text{C}$ , brittleness enhancement leads to a continuous decrease of rock resistance to deformation. The lower negative temperature also causes the intersection and initiation of numerous microcracks in the rock. Their combined effect leads to the destruction of rock specimens, and a great deal of cylindrical splitting structures are generated, which are mainly formed by the unstable expansion and intersection of numerous cracks

The failure characteristics of saturated granite under impact action show that from  $25^{\circ}\text{C}$  to  $-5^{\circ}\text{C}$ , the specimen is subjected to strong axial compression, the rock expands radially, and the tensioned part is easy to form cracks. These cracks will converge and run through to form several fracture surfaces under energy drive. With the decrease of negative temperature, the rock tends to shrink, which is

equivalent to applying precompression stress to the rock specimen. Therefore, the rock specimen has a certain ability to resist radial expansion deformation, so it can remain intact at  $-10^{\circ}\text{C}$ . However, with the further reducing negative temperature ( $-15^{\circ}\text{C}$ ), the brittleness of the rock specimen becomes more sensitive to radial contraction deformation (and becomes more sensitive with the decrease of negative temperature). Therefore, part of elastic deformation energy existed in specimen can be released, and rock particles undergo the reverse radial displacement when stress wave passes through (radial rebound contraction of the rock specimen), lamination failure then occurs in the specimen. Lower negative temperature ( $-20^{\circ}\text{C}$  to  $-40^{\circ}\text{C}$ ) results in the initiation, expansion, and intersection of a great deal of microcracks in the rock. From the perspective of damage, "frostbite" occurs at lower negative temperatures. At this time, the rock specimen will suffer tensile brittle failure under impact.

The peak stress and failure strain of granite at various temperatures  $T$  are exhibited in Figures 7 and 8.

The peak stress change of granite is quite special. The stress change is very small in the temperature range of  $25^{\circ}\text{C}$  to  $-15^{\circ}\text{C}$ . It is 159.25 MPa at  $25^{\circ}\text{C}$  and 161.53 MPa at  $-15^{\circ}\text{C}$ , respectively. Given the discretization of rock test data, the stress can be assumed to be nearly unchanged. However, as temperature declines after  $-15^{\circ}\text{C}$ , the strength property of rock begins to deteriorate, and the stress loss reaches 13.26% thus from 161.53 MPa at  $-15^{\circ}\text{C}$  to 140.11 MPa at  $-40^{\circ}\text{C}$ . Overall, the peak stress of water-saturated granite keeps constant at first and then reduces with the decreasing temperature.

The failure strain of granite reflects the change of mechanical performances of rock under the coupling action of impact load and negative temperature.

- (1) The failure strain of granite raises with the reducing temperature between  $25^{\circ}\text{C}$  and  $-5^{\circ}\text{C}$ , which is 0.0104 at  $25^{\circ}\text{C}$  and 0.0119 at  $-5^{\circ}\text{C}$ , increasing by 14.42%. The reason for the increase of failure strain is that the pore water inside the rock reaches critical saturation, and the frost heaving force resulted from water-ice phase transformation intensifies the damage degree inside the rock, increasing in failure strain value
- (2) In the range of  $-5^{\circ}\text{C}$  to  $-10^{\circ}\text{C}$ , the value of failure strain decreases sharply, which is owing to the rock matrix and ice shrink as the temperature reduces, and the microcracks and secondary defects caused by damage close with the shrinkage of volume. The rock tends to be brittle as a whole, and its ability to resist deformation decreases. Between  $-10^{\circ}\text{C}$  and  $-15^{\circ}\text{C}$ , the shrinkage rate of granite matrix and ice is the same, and the stability of the resistance to deformation of granite in this temperature range keeps the value of failure strain constant
- (3) The failure strain raises as the temperature decreases between  $-15^{\circ}\text{C}$  and  $-40^{\circ}\text{C}$ . At  $-15^{\circ}\text{C}$ , the shrinkage rate difference between rock matrix and ice becomes

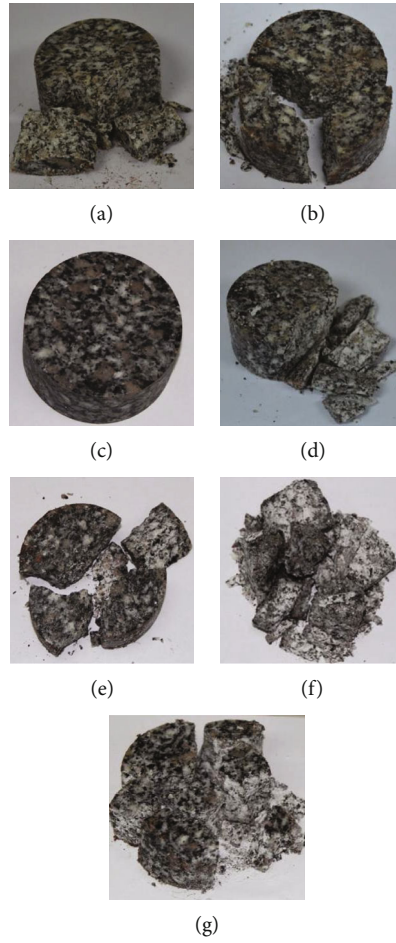


FIGURE 6: Impact failure pattern of granite: (a) 25°C; (b) -5°C; (c) -10°C; (d) -15°C; (e) -20°C; (f) -30°C; (g) -40°C.

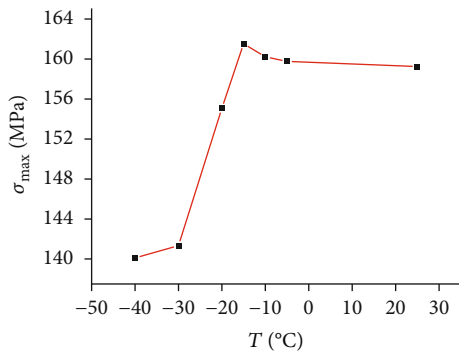


FIGURE 7: Peak stress vs. temperature for granite.

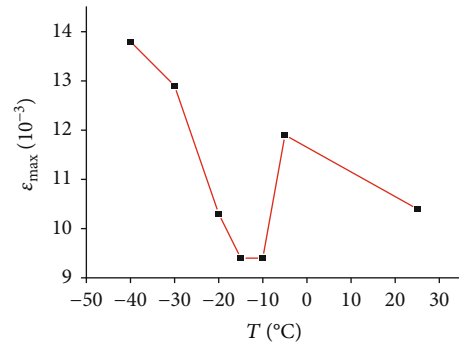


FIGURE 8: Failure strain vs. temperature for granite.

larger (the shrinkage rate of rock is larger than that of ice at -15°C). The difference of shrinkage between ice and the rock matrix intensifies the degree of damage and amplifies the influence of internal frost heaving force. The bearing capacity of rock decreases, whereas the degree of fracture intensifies, and the failure strain increases

reflected energy  $W_R$  as well as incident energy  $W_I$  of each specimen in the SHPB system could be acquired, and the corresponding dissipated energy  $W_L$  was acquired by Equation (4).

$$W_I = \left( \frac{A_b C_b}{E_b} \right) \int \sigma_I^2 dt, \quad (1)$$

$$W_R = \left( \frac{A_b C_b}{E_b} \right) \int \sigma_R^2 dt, \quad (2)$$

3.3. Energy Transfer and Dissipation Characteristics. In accordance with the dynamic impact tests, according to system energy analysis [13], the transmitted energy  $W_T$ ,

TABLE 2: Average energy statistics with various temperatures in the SHPB system for granite.

$T$ °C	$W_I$ J	$W_R$ J	$W_T$ J	$W_L$ J	SEA J·cm <sup>-3</sup>
25	528.1	75.1	399.0	54.0	0.33
-5	538.4	75.9	395.3	67.2	0.41
-10	507.6	52.7	420.0	34.9	0.21
-15	478.9	42.6	376.3	60.0	0.36
-20	516.7	80.2	315.5	121.0	0.73
-30	545.8	112.9	280.9	152.0	0.92
-40	553.2	118.6	254.2	180.4	1.09

$$W_T = \left( \frac{A_b C_{bt}}{E_{bt}} \right) \int \sigma_T^2 dt, \quad (3)$$

$$W_L = W_I - (W_R + W_T). \quad (4)$$

In the formula,  $A_b$ ,  $C_b$ , and  $E_b$  are the cross-sectional area, elastic longitudinal wave velocity, and elastic modulus of the input bar, respectively.  $\sigma_I$ ,  $\sigma_R$ , and  $\sigma_T$  are the stress time history of incident, reflected, and transmitted stress waves, respectively.  $C_{bt}$  and  $E_{bt}$  are the elastic compressional wave velocity and elastic modulus of the output rod, respectively.  $t$  is time.

Table 2 summarized the data provided by SHPB dynamic impact tests and Equations (1)–(4).

Figure 9 is drawn based on the data in Table 2 and Equations (3) and (4).

Figure 9 shows the variation trend of the transmitted and dissipated energy of granite with temperature. From the figure, it can be found that the transmitted and dissipated energy does not change much from 25°C to -10°C. The transmitted energy increases from 399 J at 25°C to 420 J at -10°C with an increase of only 5%. From -10°C to -40°C, the transmitted energy reduces gradually as the temperature decreases, from 420 J at -10°C to 254.2 J at -40°C, decreasing by 39.48%. The dissipated energy is opposite to the transmitted energy, which increases with the decrease of temperature. From -10°C to -40°C, the dissipated energy increases more than 4 times. The dynamic mechanical properties of granite from 25°C to -10°C are not significantly affected by temperature, but with the further decrease of temperature, its dynamic mechanical properties deteriorate and the anti-deformation ability declines, so the granite is more likely to be broken under dynamic load.

**3.4. Influence of Negative Temperature on Damage Variables under Impact.** The formula [21, 22] for calculating the total dissipated energy density of rock specimens under impact load is as follows:

$$w_d = \frac{W_L}{V}, \quad (5)$$

where  $W_L$  and  $w_d$  represent the total dissipated energy of rock impact failure together with the total dissipated energy density;  $V$  denotes the specimen volume.

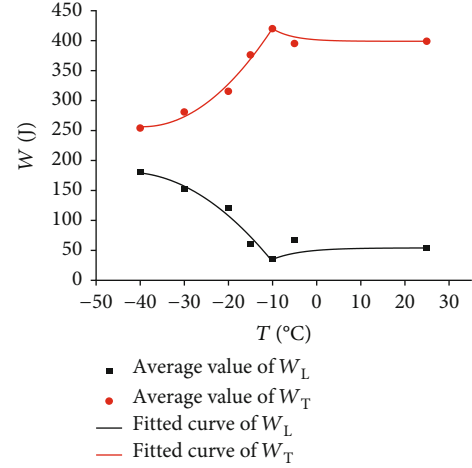


FIGURE 9: Transmitted, dissipated energy vs. temperature for granite.

TABLE 3: Damage variable vs. temperatures under dynamic impact for granite.

$T$ °C	$U$ J·m <sup>-3</sup>	$w_d$ J·m <sup>-3</sup>	$d$
25	1733390	326114.6	0.19
-5	1747300	405831.6	0.23
-10	1431270	210766.7	0.15
-15	1729900	362349.6	0.21
-20	1547010	730738.4	0.47
-30	1753010	917952.3	0.52
-40	1716760	1089464	0.63

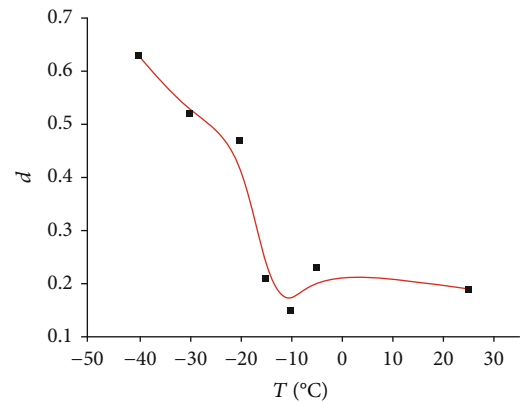


FIGURE 10: Damage variable vs. temperature under dynamic impact.

The area surrounded by the rock stress-strain curve in SHPB dynamic impact test is considered as the total absorption energy density  $u$  of rock deformation and failure:

$$u = \int \sigma d\varepsilon. \quad (6)$$

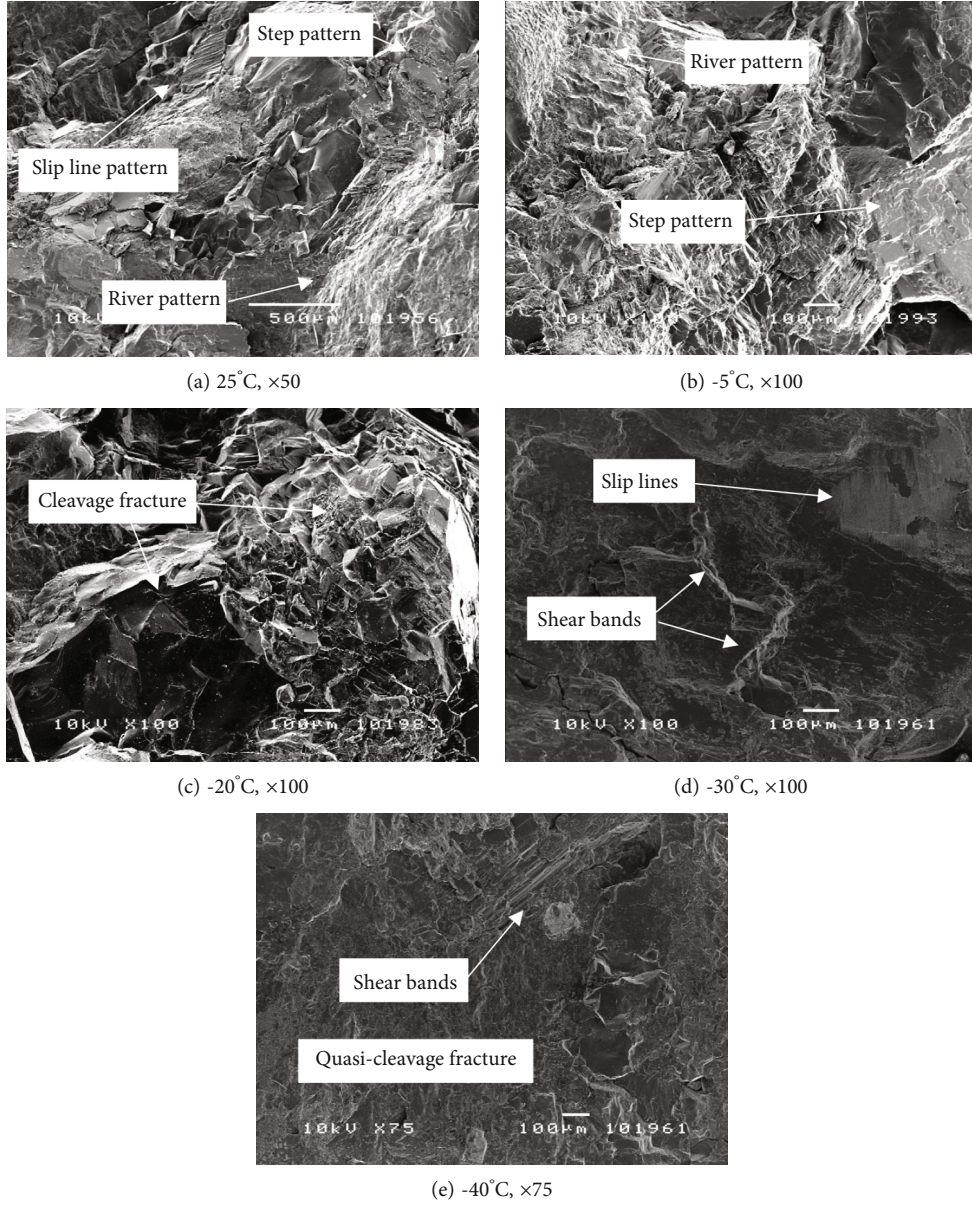


FIGURE 11: Fracture morphology of granite in different temperatures.

With the aim of analyzing the effect of different temperatures on rock dynamic damage, damage variable  $d$  represented by the energy concept is introduced.

$$d = \frac{w_d}{u}, \quad (7)$$

where  $w_d$  and  $u$  represent the total dissipated energy density and total absorbed energy density of rock deformation and failure under impact load, respectively.

Based on Equations (5)–(7), the damage variables of granite specimens under impact load are counted [13], as reflected in Table 3, along with corresponding negative temperature parameters.

The variation range of damage variables represented by energy density is relatively small (0.15 to 0.23) under the coupling effect of a negative mild impact is in the range of

25°C to -10°C, but corresponding to the macroscopic failure characteristics of rock is the difference between integrity and fracture. Then, with the decrease of negative temperature (-10°C to -40°C), the value of the damage variable continues to increase (0.15 to 0.63), and the degree of specimen breakage intensifies, which is in accordance with the macrofailure features of granite. The damage variable  $d$  and temperature  $T$  were fitted, and the functional expression (see Equation (8)) reflecting the relationship between them was obtained as shown in Figure 10.

$$d = -4.83795e^{-4}T^2 - 0.04041T - 0.22134, R^2 = 0.91158, T \in [-40, -10]. \quad (8)$$

3.5. Analysis of the Influence of Negative Temperature on Dynamic Mechanical Properties of Granite. Based on the

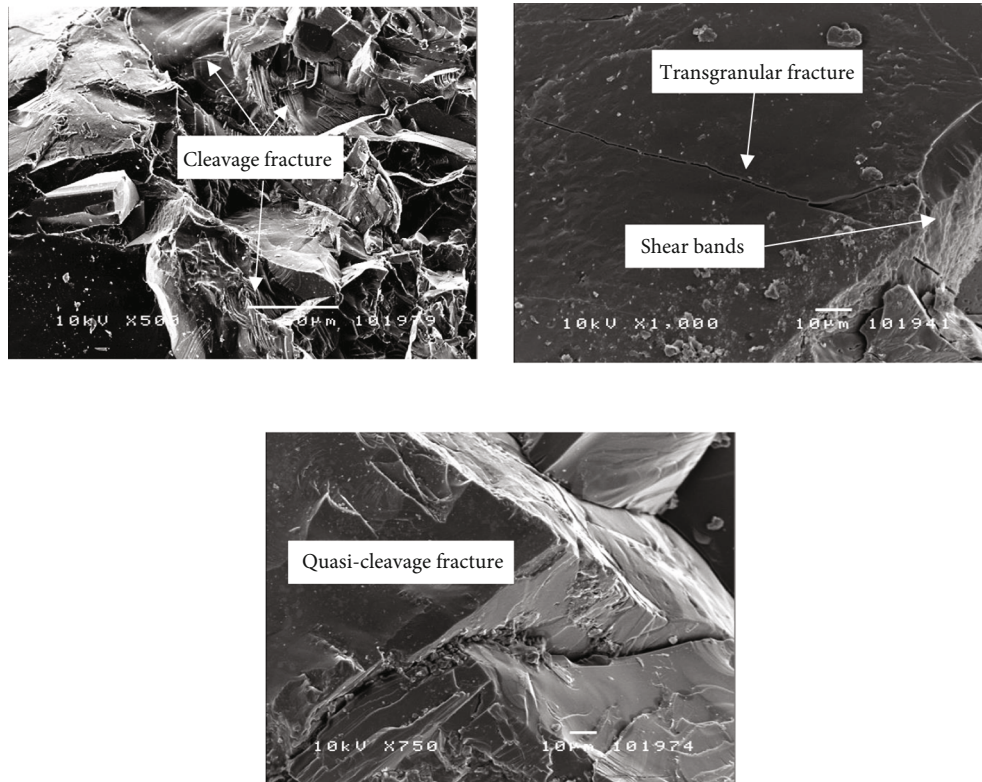


FIGURE 12: Local fracture morphology of frozen granite from  $-20^{\circ}\text{C}$  to  $-40^{\circ}\text{C}$ .

analysis, it can be determined that low negative temperature (in this series of tests, it means the temperature after dropping to  $-20^{\circ}\text{C}$ ) will cause “frostbite” in granite under high strain rate, that is, the dynamic compressive strength and bearing capacity of granite will decrease, which is called “frostbite effect” under high strain rate. Many researchers [14–20] conducted a large number of negative temperature loading tests on rocks under static or quasistatic conditions. However, the results showed that even when the temperature dropped to  $-160^{\circ}\text{C}$ , there was no “frostbite” phenomenon of strength decline occurred, which indicates that the occurrence of frostbite is related to the loading method, and the frostbite effect will occur only in the combination of negative temperature and high strain rate loading.

To some extent, the water-ice phase transformation will deteriorate the dynamic strength of water-saturated granite, which does not occur in the static load test, indicating that the rock bearing capacity under high strain rate is more sensitive to microcracks, microvoids, and other defect structures. However, in static or quasistatic cases, due to long loading time and low strain rate, the rock has a relatively long compaction stage (or crack closure stage), and it is not so sensitive to the emergence of microdefect structure, which is reflected in the macroscopic view that its strength does not decrease significantly. This insensitivity to microdefect structure becomes more obvious when the temperature is lower than  $-20^{\circ}\text{C}$ . Under a high strain rate loading, the dynamic compressive strength for the granite begins to decline at  $-20^{\circ}\text{C}$  and is more obvious and prominent at  $-30^{\circ}\text{C}$  and  $-40^{\circ}\text{C}$ , while its static strength continues to increase, and even increases faster at lower negative

temperature [21, 22]. In this study, it is found that after  $-20^{\circ}\text{C}$ , the granite dynamic mechanical strength attenuates, because the overall property of granite tends to be brittle after this temperature, and different materials (such as mineral particles, cemented materials, and solid ice) in the rock have great differences in shrinkage rate and shrinkage amplitude when they are cooled. Therefore, a large number of secondary defects such as micropores and microcracks are produced at the contact interface of the components. These secondary defects have poor plastic deformation ability under the effect of negative temperature. Under the loading of a high strain rate and low stress, brittle failure often occurs directly without any deformation, thus causing a sharp decrease in the bearing capacity and strength of granite. Under static or quasistatic loading, the negative temperature will also generate secondary defects in the rock. However, because under negative temperature, rocks have enough time for defects to close during a longer loading time, even if there is a local microscopic fracture, a lower negative temperature can make the rock shrink and tightly restrain its development. Therefore, it is impossible for high strain rate instantaneous loading to occur (under high strain rate loading in low-temperature brittle media, cracks are usually quite unstable and difficult to suppress).

#### 4. The Influence of Negative Temperature of Granite Fracture Morphology

The fracture morphology of the water-bearing granite under various temperatures was found, as revealed in Figure 11.



The fracture morphology of granite at 25°C is complex [23, 24], including river patterns formed by crystal cleavage, slip line patterns, and micropit patterns left by crystal slip on the section. Generally, the fracture morphology of granite at 25°C is diverse and slightly rough. As the temperature decreases and enters the negative temperature domain, the fracture of granite in the range of -5°C to -20°C is a mainly brittle fracture, and the river and step pattern increase gradually. The slip separation occurs in some areas due to shear deformation, and the shear band pattern and stripe pattern appear. After -20°C, the characteristics of rock slip separation caused by shear deformation become more obvious, and a large number of shear bands, slip lines, and flat surface patterns appear in the mesofracture morphology.

As shown in Figure 12, the negative temperature from -20°C to -40°C possesses an evident effect against the fracture morphology of granite. The granite exhibits certain frost brittleness at negative temperatures. Compared with 25°C, the proportion of step pattern and river pattern in fracture morphology increases at -20°C, and the slip line pattern also appears in large quantity. As the negative temperature continues to decrease (-30°C to -40°C), the slip separation phenomenon increases, and a large number of shear band patterns and quasicleavage fractures appear on the section. At the same time, there are very obvious cracks, which are derived from secondary defects [25–28]. The lower negative temperature will lead to the formation of secondary defects such as microcracks among the mineral particles in granite. These cracks have poor plastic deformation ability and are easy to destabilize and expand under high strain rate loading [29–37]. Moreover, the coupling effect of impact and negative temperature will cause the cleavage of some crystalline minerals. Finally, low stress brittle failure occurs along the granite fracture and cleavage plane.

## 5. Conclusions

The lower negative temperature will cause “frostbite” of granite, which is manifested by the decrease of dynamic strength, the increase of damage variable value, and the decrease of bearing capacity under impact. The fracture morphology shows that the negative temperature granite tends to be brittle as a whole. With the decrease of negative temperature, its fracture behavior gradually changes from cleavage fracture to transgranular fracture, and the failure mode also changes from tensile failure to shear failure.

- (1) Negative temperature brings some special changes to the dynamic mechanical properties of granites. Negative temperature is equivalent to applying precompression stress to granite. Although the rock tends to be brittle as a whole, its ability to resist tensile stress is also enhanced. Therefore, the dynamic compressive strength has little change in the range of 25°C to -15°C. However, the lower negative temperature (-20°C to -40°C) will lead to “frostbite” of granite under high strain rate loading, that is, a great deal of microcracks occur inside the rock at negative temperature and its dynamic mechanical properties

deteriorate. In the present study, after -20°C, the granite dynamic compressive strength sharply reduces, which is different from the results obtained in static or quasistatic tests

- (2) The macroscopic failure characteristics of frozen granite reveals that from 25°C to -5°C, the specimen is subjected to strong axial compression, the rock expands radially, and the part with strong tension expands easily into several fracture planes. As the negative temperature decreases, the rock tends to shrink, so the specimen has a certain ability to resist radial expansion deformation, so it can remain intact under impact action at -10°C. However, with the further decrease of the negative temperature (-15°C), the brittleness of the rock specimen is enhanced. Part of elastic deformation energy existed in specimen can be released, and rock particles generate the reverse radial displacement when stress wave passes through, and the lamellar failure occurs in the specimen. The lower negative temperature (-20°C to -40°C) enhances the initiation of microcracks inside the rock, and the rock under impact will produce tensile brittle failure
- (3) Negative temperature possesses an important effect against the fracture morphology of granite. From -5°C to -20°C, the granite is a mainly brittle fracture, and the fracture morphology is mainly river pattern and step cleavage. After -20°C, the rock is prone to shear deformation under the impact, and the shear band pattern, parallel slip line pattern, and flat plane pattern caused by slip separation appear in large numbers. The analysis of fracture morphology indicates that the lower negative temperature leads to the formation of cracks among the mineral particles in the granite. These cracks have poor plastic deformation ability and are easy to destabilize and expand under high strain rate loading. Furthermore, the coupling effect of impact and negative temperature will cause cleavage of some crystalline minerals, eventually resulting in granite’s low-stress brittle failure

## Data Availability

The experiment data used to support the findings of this study are included within the article.

## Disclosure

The funder has no role in the research design; in collecting, analyzing, or interpreting the data; when writing the manuscript; and when deciding to publish the results.

## Conflicts of Interest

The authors state that they have no conflict of interest.

## Authors' Contributions

Y.Y. is responsible for conceptualization, methodology, validation, data curation, visualization, and writing—original draft preparation; Y.Y. and J.W. for investigation; all authors for writing—review and editing; and J. W. and Y.Y. for supervision, project administration, and funding acquisition. All authors have read and agreed to the published version of the manuscript.

## Acknowledgments

The authors would like to thank the China University of Mining and Technology (Beijing), for providing instruments to conduct the research. What is more, this study was supported by the Youth Project of Beijing Natural Science Foundation (8224086).

## References

- [1] Q. S. Liu, S. B. Huang, Y. S. Kang, and X. Z. Cui, "Advance and review on freezing-thawing damage of fractured rock," *Chinese Journal of Rock Mechanics and Engineering*, vol. 34, no. 3, pp. 452–471, 2015.
- [2] W. Z. Chen, X. J. Tan, H. D. Yu, K. K. Yuan, and S. C. Li, "Advance and review on thermo-hydro-mechanical characteristics of rock mass under condition of low temperature and freeze-thaw cycles," *Chinese Journal of Rock Mechanics and Engineering*, vol. 30, no. 7, pp. 1318–1336, 2011.
- [3] K. Aoki, K. Hibiya, and T. Yoshida, "Storage of refrigerated liquefied gases in rock caverns: characteristics of rock under very low temperatures," *Tunnelling and Underground Space Technology*, vol. 5, no. 4, pp. 319–325, 1990.
- [4] T. Yamabe and K. M. Neaupane, "Determination of some thermo-mechanical properties of Sirahama sandstone under subzero temperature condition," *International Journal of Rock Mechanics and Mining Sciences*, vol. 38, no. 7, pp. 1029–1034, 2001.
- [5] R. D. Dwivedi, A. K. Soni, R. K. Goel, and A. K. Dube, "Fracture toughness of rocks under sub-zero temperature conditions," *International Journal of Rock Mechanics and Mining Sciences*, vol. 37, no. 8, pp. 1267–1275, 2000.
- [6] M. M. Tang, Z. Y. Wang, Y. L. Sun, and J. Ba, "Experimental study of mechanical properties of granite under low temperature," *Chinese Journal of Rock Mechanics and Engineering*, vol. 29, no. 4, pp. 787–794, 2010.
- [7] G. M. Xi, G. S. Yang, L. Pang, X. T. Lv, and F. L. Liu, "Experimental study on basic mechanical behaviors of sandy mudstone under low freezing temperature," *Journal of China Coal Society*, vol. 39, no. 7, pp. 1262–1268, 2014.
- [8] G. Xu, Q. Liu, W. Peng, and X. Chang, "Experimental study on basic mechanical behaviors of rocks under low temperatures," *Chinese Journal of Rock Mechanics and Engineering*, vol. 25, no. 12, pp. 2502–2508, 2006.
- [9] G. S. Yang and X. T. Lü, "Experimental study on the sandy mudstone mechanical properties of shaft sidewalls under the frozen conditions," *Journal of Mining and Safety Engineering*, vol. 29, no. 4, p. 492, 2012.
- [10] G. S. Yang, J. M. Xi, H. J. Li, L. Cheng, and X. T. Lv, "Experimental study on the mechanical properties of soft rock of coal mine shaft sidewalls under the frozen conditions," *Chinese Journal of Underground Space and Engineering*, vol. 8, no. 4, p. 690, 2012.
- [11] J. Wang, T. Zuo, X. Li, Z. Tao, and J. Ma, "Study on the fractal characteristics of the pomegranate biotite schist under impact loading," *Geofluids*, vol. 2021, Article ID 1570160, 8 pages, 2021.
- [12] M. Yongye, X. Li, J. Wang, and Z. Leng, "Research on the mechanical properties and energy consumption transfer law of cement tailings backfill under impact load," *Science of Advanced Materials*, vol. 13, no. 5, pp. 889–898, 2021.
- [13] Y. B. Wang, Y. Yang, Y. T. Zhang, and J. G. Wang, "Dynamic mechanical properties of coals subject to the low temperature-impact load coupling effect," *Scientific Reports*, vol. 9, no. 1, p. 20218, 2019.
- [14] S. Renliang, Y. A. N. G. Hao, Z. H. A. N. G. Jinxun, G. U. O. Zhiming, and Z. H. A. O. Dinghong, "Mechanical properties of saturated red sandstone of Meilinmiao mine under loading and unloading at negative temperatures," *Journal of Mining and Safety Engineering*, vol. 33, no. 5, p. 924, 2016.
- [15] R. L. Shan, H. Yang, Z. M. Guo, X. Liu, and L. Song, "Experimental study of strength characters of saturated red sandstone on negative temperature under triaxial compression," *Chinese Journal of Rock Mechanics and Engineering*, vol. 33, pp. 3657–3664, 2014.
- [16] R. L. Shan, L. Zhang, H. Yang, J. X. Zhang, and Z. M. Guo, "Experimental study of freeze-thaw properties of saturated red sandstone," *Journal of China University of Mining and Technology*, vol. 45, no. 5, p. 923, 2016.
- [17] H. J. Li, *Experimental Study on Rock Mechanical Properties under Freezing Conditions*, Xi'an University of Science and Technology, Xi'an, 2009.
- [18] L. Cheng, *Experimental Study on Rock Mechanical Properties under Freezing Conditions and Application in Project*, Xi'an University of Science and Technology, Xi'an, 2009.
- [19] J. M. Xi, G. S. Yang, and X. H. Dong, "Effect of freezing temperature on mechanical properties of sandy mudstone," *Journal of Chang'an University (Natural Science Edition)*, vol. 34, no. 4, p. 92, 2014.
- [20] Y. P. Li and Z. Y. Wang, "Uniaxial compressive mechanical properties of rock at low temperature," *Journal of University of Science and Technology Beijing*, vol. 33, no. 6, pp. 671–675, 2011.
- [21] J. Y. Xu, J. S. Fan, and X. C. Lü, *Dynamic Mechanical Properties of Rock with the Confining Pressure*, Northwestern Polytechnical University Press, Xi'an, 2012.
- [22] H. P. Xie, F. Gao, H. W. Zhou, and J. P. Zuo, "Fractal fracture and fragmentation in rocks," *Journal of Disaster Prevention and Mitigation Engineering*, vol. 23, no. 4, p. 1, 2003.
- [23] Y. Qian, *Experimental Study on Blasting Fragment-Size of Joints Rock Mass Based on Fractal Theory*, Wuhan University of Technology, Wuhan, 2005.
- [24] M. Wen, J. Y. Xu, H. Y. Wang, X. Y. Fang, and G. H. Zheng, "Fractography analysis of sandstone failure under low temperature-dynamic loading coupling effects," *Chinese Journal of Rock Mechanics and Engineering*, vol. 36, no. 2, pp. 3822–3830, 2017.
- [25] J. G. Wang, Y. Liu, and K. G. Li, "Dynamic characteristics of deep dolomite under one-dimensional static and dynamic loads," *Journal of The Institution of Engineers (India): Series A*, vol. 101, no. 1, pp. 49–56, 2019.
- [26] P. Wang, J. Y. Xu, S. Liu, H. Y. Wang, and S. H. Liu, "Static and dynamic mechanical properties of sedimentary rock after

- freeze-thaw or thermal shock weathering,” *Engineering Geology*, vol. 210, pp. 148–157, 2016.
- [27] P. Wang, J. Y. Xu, S. H. Liu, and H. Y. Wang, “Dynamic mechanical properties and deterioration of red-sandstone subjected to repeated thermal shocks,” *Engineering Geology*, vol. 212, pp. 44–52, 2016.
- [28] P. V. Nikolenko, S. A. Epshtein, V. L. Shkuratnik, and P. S. Anufrenkova, “Experimental study of coal fracture dynamics under the influence of cyclic freezing-thawing using shear elastic waves,” *International Journal of Coal Science & Technology*, vol. 8, no. 4, pp. 562–574, 2021.
- [29] K. Bo-Hyun, W. Gabriel, M. K. Larson, and B. Steve, “Investigation of the anisotropic confinement-dependent brittleness of a Utah coal,” *Science and Technology*, vol. 8, no. 2, pp. 274–290, 2021.
- [30] G. Wu, K. Liu, W. R. Hu, J. C. Li, S. Dehkhoda, and Q. B. Zhang, “Quantification of dynamic damage and breakage in granite under confined indentation,” *International Journal of Rock Mechanics and Mining Sciences*, vol. 144, p. 104763, 2021.
- [31] Z. Song, Y. Wang, H. Konietzky, and X. Cai, “Mechanical behavior of marble exposed to freeze-thaw-fatigue loading,” *International Journal of Rock Mechanics and Mining Sciences*, vol. 138, p. 104648, 2021.
- [32] Y. Zhou, D. Zhao, B. Li, H. Wang, Q. Tang, and Z. Zhang, “Fatigue damage mechanism and deformation behaviour of granite under ultrahigh-frequency cyclic loading conditions,” *Rock Mechanics and Rock Engineering*, vol. 54, no. 9, pp. 4723–4739, 2021.
- [33] Y. Yang, N. Zhang, and J. Wang, “A study on the dynamic strength deterioration mechanism of frozen red sandstone at low temperatures,” *Minerals*, vol. 11, no. 12, p. 1300, 2021.
- [34] Y. Yang, N. Zhang, and J. Wang, “Fracture morphology analysis of frozen red sandstone under impact,” *Shock and Vibration*, vol. 2021, Article ID 4388132, 12 pages, 2021.
- [35] X. Liu, S. Song, Y. Tan et al., “Similar simulation study on the deformation and failure of surrounding rock of a large section chamber group under dynamic loading,” *International Journal of Mining Science and Technology*, vol. 31, no. 3, pp. 495–505, 2021.
- [36] A. I. Lawal, S. Kwon, O. S. Hammed, and M. A. Idris, “Blast-induced ground vibration prediction in granite quarries: an application of gene expression programming, ANFIS, and sine cosine algorithm optimized ANN,” *Mining Science and Technology*, vol. 31, no. 2, pp. 265–277, 2021.
- [37] Z. Zhang, Q. Qian, H. Wang et al., “Study on the dynamic mechanical properties of metamorphic limestone under impact loading,” *Lithosphere*, vol. 2021, no. Special 4, article 8403502, 2021.